Published online 27 October 2011 *Nucleic Acids Research, 2012, Vol. 40, No. 4* ***1841–1855***
doi:10.1093/nar/gkr872

Solution structure and stability of the DNA undecamer duplexes containing oxanine mismatch

Seung Pil Pack[1,*], Hirohisa Morimoto[2], Keisuke Makino[3], Kunihiko Tajima[2] and Kenji Kanaori[2,*]

[1]Department of Biotechnology and Bioinformatics, Korea University, Jochiwon, Chungnam 339-700, Korea, [2]Department of Biomolecular Engineering, Kyoto Institute of Technology, Matsugasaki, Sakyo-ku, Kyoto 606-8585 and [3]Office of Society-Academic Collaboration for Innovation, Kyoto University, Yoshida-Honmachi, Kyoto 606-8501, Japan

Received July 5, 2011; Revised September 27, 2011; Accepted September 30, 2011

ABSTRACT

Solution structures of DNA duplexes containing oxanine (Oxa, O) opposite a cytosine (O:C duplex) and opposite a thymine (O:T duplex) have been solved by the combined use of ^{1}H NMR and restrained molecular dynamics calculation. One mismatch pair was introduced into the center of the 11-mer duplex of [d(GTGAC$\underline{O}_6$CACTG)/d(CAGT G$\underline{X}_{17}$GTCAC), X = C or T]. ^{1}H NMR chemical shifts and nuclear Overhauser enhancement (NOE) intensities indicate that both the duplexes adopt an overall right-handed B-type conformation. Exchangeable resonances of C_{17} 4-amino proton of the O:C duplex and of T_{17} imino proton of O:T duplex showed unusual chemical shifts, and disappeared with temperature increasing up to 30°C, although the melting temperatures were >50°C. The O:C mismatch takes a wobble geometry with positive shear parameter where the Oxa ring shifted toward the major groove and the paired C_{17} toward the minor groove, while, in the O:T mismatch pair with the negative shear, the Oxa ring slightly shifted toward the minor groove and the paired T_{17} toward the major groove. The Oxa mismatch pairs can be wobbled largely because of no hydrogen bond to the O1 position of the Oxa base, and may occupy positions in the strands that optimize the stacking with adjacent bases.

INTRODUCTION

DNA polymerase makes errors by misincorporating natural DNA bases and base analogs. Because of the wide variety of possible mismatches and the varying efficiency with which they are repaired, structural studies are necessary to understand in detail how these mismatch pairs differ and can be distinguished from standard Watson–Crick base pairs. Duplex structures with various mismatch pairs of natural bases, such as A:C (1–4), G:T (5–7), have been reported and effects of the mismatch on the structures and biological implications have been extensively studied (8). And also, various unusual mismatch pairs have been studied by X-ray crystallography and NMR to explain their mutagenic properties.

Oxanosine (5-amino-3-β-$_D$-ribofuranosyl-3*H*-imidazo [4,5-*d*]oxazin-7-one) was originally isolated from *Streptomyces capreolus* MG265-CF3 and has antibiotic properties in both its ribo and 2′-deoxyribo forms (9). Oxanine (Oxa, O) is a unique deaminated base in which an endocyclic nitrogen atom of guanine is substituted by an oxygen atom. It was reported that 2′-deoxyoxanosine (dOxa, Figure 1A) was produced by the reaction of 2′-deoxyguanosine with nitric oxide (NO)- or nitrous acid (HNO_2)-induced nitrosative oxidation (10). Since Oxa, which is a DNA lesion of guanine, could be produced in the cellular system by NO, HNO_2 or other nitrosating agent, its genotoxic properties including deglycosylation susceptibility, base pairing stability and base incorporation patterns have been analyzed (11,12). Cytosine (Cyt) and thymine (Thy) were incorporated by *Escherichia coli* Klenow Fragment to pair with Oxa in a DNA template with similar efficiency. If Oxa is formed in DNA strands, dOxa can exist for a sufficient time since dOxa moiety is not easily hydrolyzed due to its stable *N*-glycosidic bond between base and sugar moieties. Therefore, the Oxa generated in cellular genomes may induce the misincorporation of incorrect nucleotides causing G:C to A:T transition.

On the basis of the chemical structure, Oxa was expected to form two hydrogen bonds with either Cyt or Thy (11). By measuring melting temperatures (T_m) and thermodynamic parameters, the base pair of O:C showed relatively high stability in DNA duplexes

*To whom correspondence should be addressed. Tel: +82 41 860 1419; Fax: +82 41 864 2665; Email: spack@korea.ac.kr
Correspondence may also be addressed to Kenji Kanaori. Tel/Fax: +81 75 724 7825; Email: kanaori@kit.ac.jp

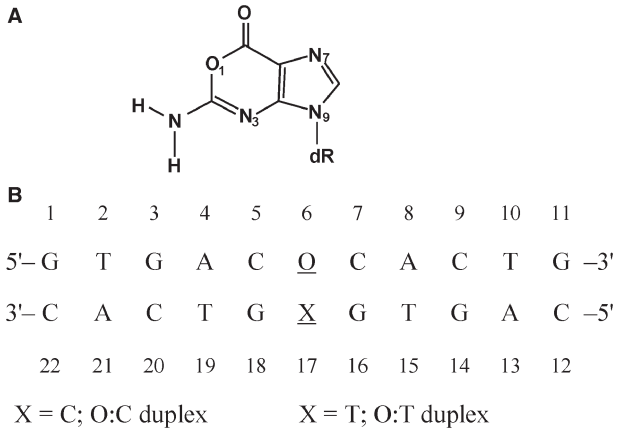

Figure 1. Chemical structures analyzed in the study. (**A**) Structures of 2′-deoxyoxanosine and (**B**) DNA sequence contexts of the O:C duplex.

compared with other base combinations. The orders were O:C > O:T > O:A > O:G (13). In terms of the most stable mismatch of O:C, two models have been proposed for this interaction: a Watson–Crick geometry involving two hydrogen bonds and a wobble geometry. A wide range of theoretical methods have been used to analyze the mutagenic properties of Oxa (14). The theoretical study have focused on the stability of the Oxa mismatch pairs in DNA: Molecular dynamics (MD) simulation showed that the d(G:C) → d(O:C) mutation increases the flexibility of the hydrogen bonded dimer, which fluctuates between the co-existence of different binding modes calculated in the gas phase (14). By examining the cleavage of oligodeoxyribonucleotides containing Oxa by bacterial endonuclease V, hypothetic models of Oxa-containing base pairs and deaminated base recognition mechanism were also proposed (15). However, there has not been as of yet consensus on its structure, because structural studies on DNA oligomers containing the O:C mismatch have not been carried out by NMR or X-ray crystallography so far on account of difficulties in preparing a dOxa amidite monomer. Since the monomer has been successfully synthesized and employed to the automatic DNA synthesizer (13,16), it has become possible to investigate how the mismatch of Oxa base pair affects the structure and properties of the Oxa duplexes at an atomic resolution. Recently, biotechnological utilization of the dOxa oligonucleotides has been reported. For example, T4 DNA ligase-based mismatch detection methods have been proposed as useful strategies for single nucleotide polymorphism (SNP) analyses, and biomolecular response of oxanine in DNA strands to T4 polynucleotide kinase, T4 DNA ligase and restriction enzymes (17,18). In order to make further development of these biotechnological and biomedical utilizations, it has been more important to elucidate the mismatch structures in detail for the oligonucleotides containing Oxa.

In the present study, we have focused on the effects of the O:C and O:T mismatches on the structure and stability of DNA duplex, and examined the theoretical data obtained for the base pairing of the O:C and O:T (14). The mismatch pairs were introduced into the center of the same 11-mer DNA duplex. The DNA sequence was designed and chosen to avoid the signal overlapping and to obtain structural information around the mismatch pair. In order to obtain information about the base pairing of O:C, interstrand nuclear Overhauser enhancement (NOE) from the cytosine 4-amino group of the mismatch to exchangeable protons in the adjacent base pairs of O:C is significant because the ^{1}H–^{1}H distances between those protons are short and sensitive to the DNA conformations (19). For the O:T duplex, the structure has been mainly compared with the G:T duplex. Based on the base pairing geometry and hydrogen bond of the O:C and O:T base pair, biological implication will be discussed.

MATERIALS AND METHODS

Nomenclature

In order to avoid confusing the number of the oxanine ring atoms with those corresponding guanine, the number of the oxanine ring in the present study was changed to be the same as that of the guanine ring. The numbering system for the [d(GTGACOCACTG)/d(CAGTGXGTCAC)] is shown in Figure 1B, where O indicates an oxanosine moiety, and X is C (O:C duplex) or T (O:T duplex). The mismatch pair (O_6:X_{17}) is underlined. And the same numbering system was applied to two reference DNA duplexes, [d(GTGACGCACTG)/d(CAGTGCGTCAC)] (G:C duplex) and [d(GTGACGCACTG)/d(CAGTGTGTCAC)] (G:T duplex).

Sample preparation

The DNA strands were synthesized on an automatic synthesizer by the phosphoramidite method and purified by gel filtration and reverse phase HPLC as previously reported (13). The concentration of the NMR sample was estimated using the extinction coefficients at 260 nm which were calculated by the nearest neighbor method (13). Each duplex was dissolved at a concentration of 2 mM in a buffer containing 10 mM sodium phosphate, 100 mM NaCl and 0.2 mM ethylenediaminetetraacetic acid. The pH of the solution was adjusted to 7.0, unless otherwise stated, by the addition of HCl and NaOH. The solution was heated at 80°C for 10 min and was gradually cooled down to room temperature immediately prior to the NMR measurements.

NMR spectroscopy

NMR experiments were carried out on a Bruker ARX-500 spectrometer (500.13 MHz for ^{1}H) and JEOL JNM-ECAseries-920 (920 MHz for ^{1}H). A set of 2D NMR spectroscopy experiments [DQF-COSY (20), TOCSY (21), E-COSY (22), NOESY (23)] was obtained for the duplexes dissolved in the deuterated buffer. NOESY spectra obtained with mixing times of 50, 100 and 200 ms were measured with a 6.5 s relaxation delay. Taking the duplex stability and peak separation into account, several temperatures used for the NMR measurements were

employed between 5–25°C for the DNA duplexes. The jump-and-return NOESY (24) by the 500 MHz NMR machine and water gated NOESY (25) by the 920 MHz NMR machine were measured for the samples dissolved in the 90% H_2O/10% D_2O buffer at both pH 6.0 and 7.0 to assign labile protons and evaluate NOE cross-peak intensities for the O:T and G:T duplexes, because exchange rates of the imino proton with water is the slowest at pH 6 and that of amino protons with water at pH 7 (19). ^{1}H chemical shifts were referred to internal sodium 3-(trimethylsilyl)propionate-*2,2,3,3-d*$_4$. Acquired data were processed using the program UXNMR (Bruker) and NMRpipe (LA systems, Tokyo, Japan). The NMR sample conditions for the T_m measurements were identical to those for the 2D measurements. The 1D ^{1}H-NMR spectra were collected after the attainment of the equilibration at each temperature. The chemical shift change of well-isolated peaks was plotted as a function of temperature, and the collected data points were fitted to a sigmoidal curve by a non-linear least squares refinement procedure of ORIGIN (Microcal Software Inc.). All the T_m values were reproducible from the curves with temperature increasing and decreasing, and the standard deviations were ±0.5–1.0°C on repetitions of the experiments.

Restrained MD

The NOESY cross-peak intensities were obtained using a measure-volume tool of NMRpipe. The volumes were normalized against C H5-H6 and H2′-H2″ NOEs, which correspond to fixed distances. All the NOE restraints between the non-exchangeable protons were derived from 50-ms NOESY spectra with a long delay (6.5 s) in D_2O. The upper and lower bound corrections of the NOE restraints (a force constant of 20.0 kcal mol/Å^2) were set to be 15 and 10% of the obtained interproton distances, respectively. The sequential NOEs regarding exchangeable protons were converted to medium (3.0–4.2 Å) and weak (4.0–5.0 Å) restraints. The numbers of the interproton distances were 231 and 225 for O:C and O:T duplex, respectively. The initial A- and B-structures were generated using Maestro (Schrödinger, MA, USA). The structure calculations were done by XPLOR3.8 (26). Geometrical parameters and the atomic charges of the oxanosine residue were built by using those of the guanosine residue, and the no charge was employed on the O1 atom to avoid the effect of the force field parameters. These parameters were added to the database that was referred to during the structure calculation. Restrained molecular dynamics (rMD) and energy minimization calculations included 102 backbone torsion angle restraints with a force constant of 5.0 kcal/mol/rad^2, and six distance restraints per Watson–Crick base pair (a force constant of 50.0 kcal/mol/Å^2) to maintain Watson–Crick base pairing (27) with bounds of ±0.1 Å. For the mismatch pair, one hydrogen bond was enforced using canonical distances with bounds of ±0.1 Å between O_6 NH_2 and C_{17} N3 atom for the O:C duplex, and between O_6 NH_2 and T_{17} O2 atom for the O:T duplex. The reasons of those hydrogen bonds in the mismatch pairs will be described in the 'Results' section. The backbone angle restraints, keeping the range between the A- and B-form, were defined as previously described (28,29). The rMD calculations of 20 000 steps at 300 K were carried out with a simulated annealing protocol provided by Grünger (26) to search conformational space for structures consistent with the NMR restraints. The resulting structures were submitted to a final energy minimization, giving rise to the final structures. Seventeen structures of the O:C duplex and 15 structures of the O:T duplex were selected from 100 calculations on the basis of the lowest energy values. There were no violated distance constraints by >0.25 Å and no violated dihedral angle constraints by >5°. The helical parameters were analyzed using CURVES 5.3 (30,31).

RESULTS

Resonance assignment

Proton resonances were assigned for all the duplexes (O:C, O:T, G:T and G:C) from a complete set of homonuclear 2D NMR data using established NMR techniques for nucleic acid analyses (19). The assignment of non-exchangeable DNA protons was achieved by analyzing all regions of the NOESY spectra obtained with various mixing times in combination with DQF-COSY and TOCSY data, and H5′/5″ proton assignments were not assigned because of signal overlapping. For example, the NOESY spectrum of the O:C duplex is shown in Figure 2. The ^{1}H resonance assignments are summarized in Supplementary Table S1. All the non-exchangeable protons were sharp, indicating that no chemical exchange occurs between conformers in an NMR time scale. Intra-residue and sequential base to H1′, H2′, H2″ and H3′ cross-peaks characteristic of right-handed DNA duplex were observed for all the duplexes. These connectivities were seen throughout the duplexes, including the lesion site and surrounding residues. The intra-residue NOE intensities of the O_6 H8-H1′ and paired C_{17} H6-H1′ cross-peaks were weak, and of similar intensity as the other intraresidue aromatic-H1′ cross-peaks, suggesting that those mismatch residues are *anti*, which excludes unusual geometries such as those found in Hoogsteen or reverse-Hoogsteen base pairs. For the O:T duplex, the mismatch residues of O_6 and T_{17} also showed an *anti* conformation. The NOESY spectra of the O:C and O:T duplexes in D_2O showed intranucleotide sugar–base NOE patterns of B-form DNA [H2′(*i*)-H8/H6(*i*) >> H1′(*i*)-H8/H6(*i*) > H3′(*i*)-H8/H6(*i*)]. Well-digitized E-COSY spectra were used to measure the coupling constants. The obtained *J* coupling data ($^3J_{1'2'}$ and $^3J_{1'2'}$) were in the range of 5.4–8.0 Hz for both of the O:C and O:T duplexes. The sugar pucker and glycosidic bond conformations probably lie in the O4′-*endo* to C2′-*endo* and *anti* ranges, respectively. All the duplexes take an overall B-form DNA.

Exchangeable imino and amino proton resonances for each duplex were also assigned by measuring the samples in H_2O and by observing NOE cross-peaks between the exchangeable and non-exchangeable protons (Figure 3). The imino and amino proton cross-peaks due to

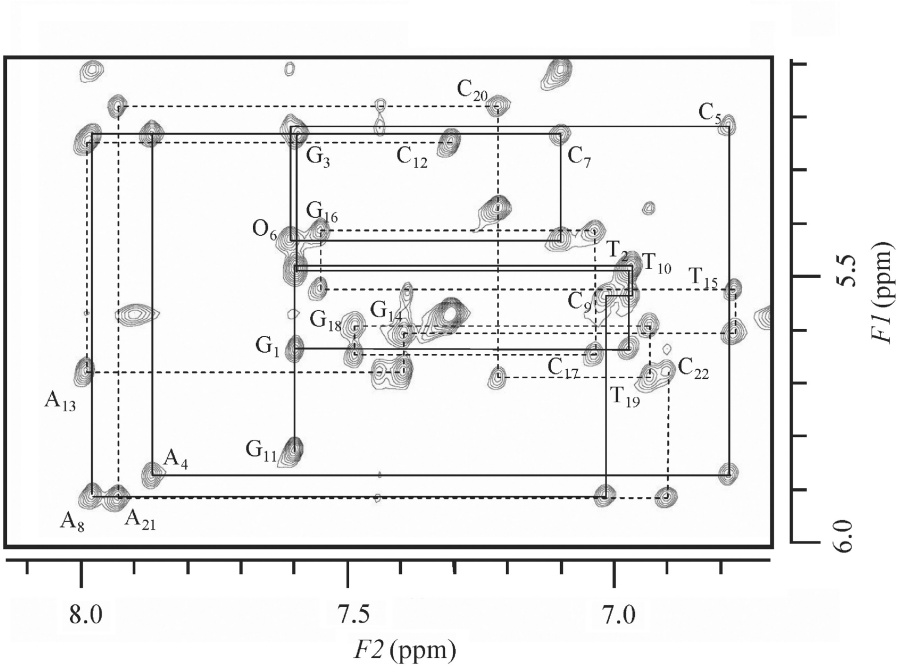

Figure 2. ^{1}H 2D-water gated NOESY spectrum (mixing time 200 ms) of the DNA duplex containing the O:C mismatch collected at 22°C. Sequential NOE connectivities for a strand of d(GTGACOCACTG) are indicated by a solid line, and those for d(CAGTGCGTCAC) are indicated by a broken line. Intraresidue NOE connectivities between H1′ and H8/H6 are indicated by residue names.

interactions with adjacent bases establish base pair formation and normal base stacking throughout the duplex. For the G:C duplex, the inter- and intrastrand imino–imino NOEs were observed through the duplex, except for the terminal imino protons. On the other hand, for the O:C duplex, the similar NOE cross-peaks were observed between the imino protons in the regions of T_2-G_3-T_{19}-G_{18} and G_{16}-T_{15}-G_{14}-T_{10} because of the absence of the imino proton in the central O:C mismatch pair. Two internal and external amino proton resonances of C_{17} (C_{17}-NH_{int} and C_{17}-NH_{ext} in Figure 3A) were separately observed at 6.43 and 9.21 ppm, respectively. The downfield resonance at 9.21 ppm should be an internal amino proton (C_{17}-NH_{int}). The C_{17}-NH_{int} resonance exhibited weak NOE cross-peaks with the G_{16}- and G_{18}-NH resonances, and also a strong and broad NOE cross-peak with the amino protons of O_6 (O_6-NH_2) at 6.47 ppm, which was overlapped with the intraresidue NOE between the C_{17}-NH_{int} and C_{17}-NH_{ext}. For the O:T duplex, the imino proton resonance of T_{17} (T_{17}-NH) was observed at 9.21 ppm (Figure 3B), and the G:T duplex exhibited two imino proton resonances of G_6 and T_{17} at 10.45 and 11.62 ppm, respectively (Figure 3C). The T_{17}-NH of the O:T duplex was shifted to the more upfield by 2.4 ppm than that of the G:T duplex which is hydrogen bonded to the opposite guanine. NOE cross-peak pattern of the G_6:T_{17} wobble pair of the G:T duplex coincides with that reported for self-complementary DNA duplex with the G:T mismatch pair (5,32,33): The G_6-NH_2 protons, observed at 5.82 ppm showed a strong NOE cross-peak with G_6-NH at 10.45 ppm, and a medium NOE cross-peak with that of T_{17}-NH at 11.62 ppm. Weak sequential NOEs were observed for the G:T duplex between the imino protons of G_{18}-T_{17}-G_{16} and G_{18}-G_6-G_{16}. For the O:T duplex, weak sequential NOEs were also observed between imino protons of the intrastrand, G_{18}-T_{17}-G_{16}. And the T_{17}-NH proton showed a medium NOE cross-peak with the O_6-NH_2 resonance. The O:T and G:T duplexes resemble each other in the NOE cross-peak pattern, although the chemical shift of the T_{17}-NH proton of the O:T duplex was different from that of the G:T duplex.

Comparison of chemical shift values between the duplexes

Chemical shift difference ($\Delta\delta$) provides a first approximation of the structure change. In order to examine the effect of the O:C and O:T mismatch on the chemical shifts, the chemical shift differences were compared with the G:C duplex (Figure 4) or to the G:T duplex (Supplementary Figure S1) that contains the wobble G:T pair. As for the non-exchangeable protons, almost all proton resonances exhibited only a small difference ($|\Delta\delta| < 0.1$ ppm). Significant chemical shift differences were observed for the protons of the positions of C_5-O_6-C_7, and G_{18}-X_{17}-G_{16}, indicating that the structure change caused by the O:C or O:T mismatch is restricted to its neighboring Watson–Crick base pairs. The comparison of the chemical shift between the duplexes showed that large differences in the chemical shift ($|\Delta\delta| > 0.2$ ppm) were observed for C_5-H2′/H2″, G_{16}-H1′ and X_{17}-H1′/H2″ (X = C or T). The non-exchangeable proton resonances of O_6 in the O:C and O:T duplexes showed almost identical chemical shifts to those corresponding of G_6 in the G:C duplex (Figure 4A and B). It is of interest that the largest differences were observed for the neighboring residue (C_5) and residues of G_{16} and C_{17} in the counter strand, but not for O_6 itself. This indicates that the introduction of Oxa

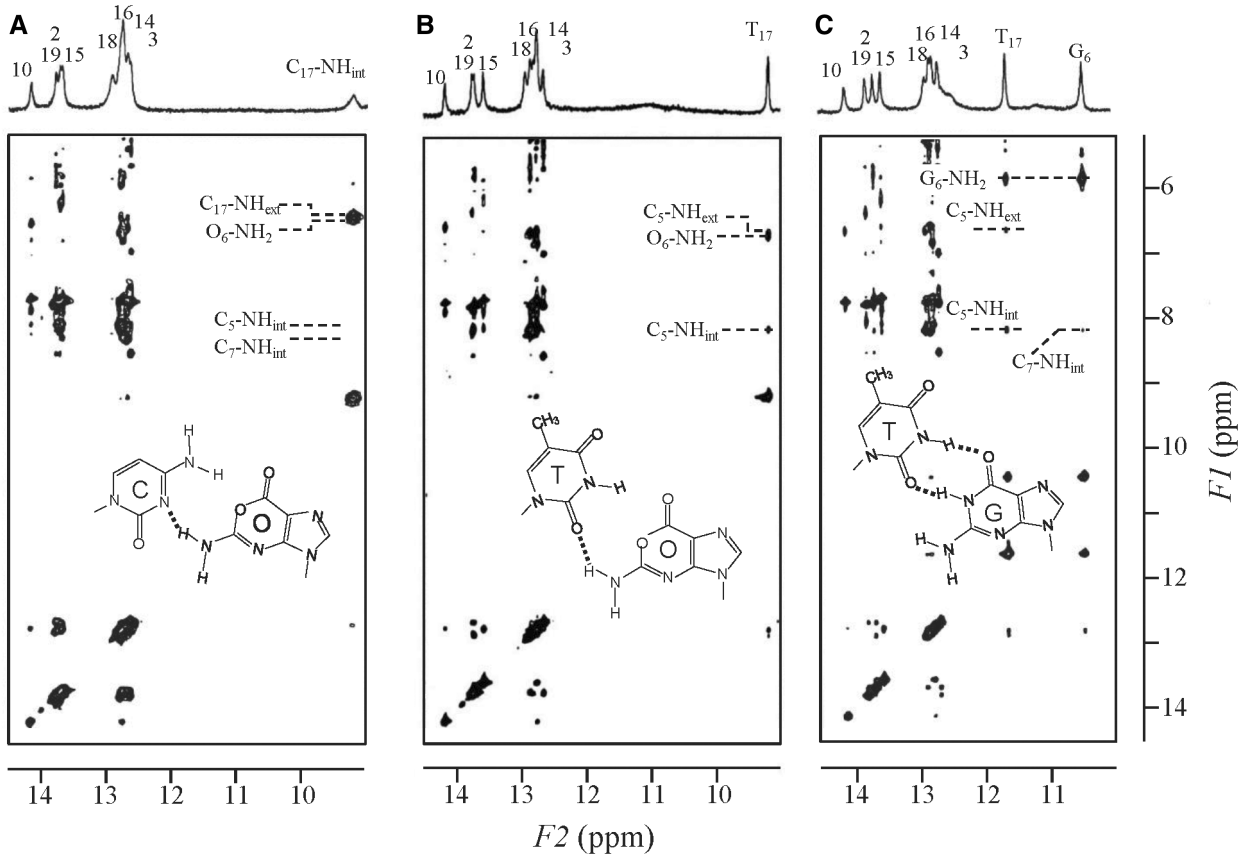

Figure 3. ^{1}H jump-and return 2D-NOESY spectra (mixing time 200 ms) of the DNA duplexes containing (**A**) O:C, (**B**) O:T and (**C**) G:T mismatches collected at 5°C. The spectrum of the O:C duplex was measured at pH 7.0, and those of the O:T and G:T at pH 6.0. There was no significant difference in the chemical shift of the non-exchangeable protons at pH 6.0 and 7.0.

influences not only base pairing with the base at the position of 17, but also the duplex structure of the adjacent residues, possibly resulting in base stacking. For the largest shifted protons, their deviations of the O:C, O:T and G:T duplexes from those of the G:C duplex are shown in Figure 5. It should be noted that the deviations of the O:C duplex from the G:C duplex is opposite to those of the O:T and G:T duplexes for the largest shifted protons. For example, C_5-H2′ showed a large upfield shift for O:C, but a downfield shift for O:T, while C_{17}-H1′ showed a downfield shift for O:C, but an upfield shift for O:T. Thus, the chemical shift differences between O:C and O:T (or G:T) were large (Figures 4C and 5), and the chemical shifts of O:T agreed more closely with those of G:T than those of O:C (Supplementary Figure S1B). Taking it into account that the G:C and G:T duplexes take a Watson–Crick and wobble geometry, respectively, the geometry of the O:T pair including its adjacent base pairs may take an intermediate geometry between them, while the O:C pair takes a different geometry.

Among exchangeable proton resonances, the C_{17}-NH_{int} proton resonance of the O:C duplex (Figure 3A) and the T_{17}-NH proton resonance of the O:T duplex (Figure 3B) showed outstanding differences between the duplexes. The C_{17}-NH_{int} proton resonance (9.21 ppm) of the O:C duplex was shifted to the downfield as compared with single-stranded cytosine amino protons (7.0–8.0 ppm) and was even downfield relative to the hydrogen-bonded cytosine amino protons in standard Watson–Crick base pairs (8.0–8.6 ppm, in Supplementary Table S1). The corresponding C_{17}-NH_{int} proton of the G:C duplex were observed at 8.28 ppm (data not shown). Therefore, the C_{17}-NH_{int} proton resonance of the O:C duplex shifted to the downfield by 1 ppm, as compared with that of the G:C duplex. This downfield shift of the C_{17}-NH_{int} proton resonance involved in the mismatched base pair suggests that the base pairing geometry is different from the canonical Watson–Crick of G:C. On the other hand, the imino proton of T_{17} of the O:T duplex was shifted to the upfield by 2.5 ppm, as compared with that of the G:T duplex. Thus, between the O:T and G:T duplexes, the large difference was only observed for T_{17}-NH although there are small differences for all the non-exchangeable protons, indicating that the hydrogen bond pattern of O:T base pair is different from the reported wobble pattern of G:T, while the duplex structures resemble each other.

Melting profile of the O:C and O:T duplex

In order to examine whether the stability of the duplexes could correlate with the structural differences, thermal melting profile was investigated for all the duplexes by

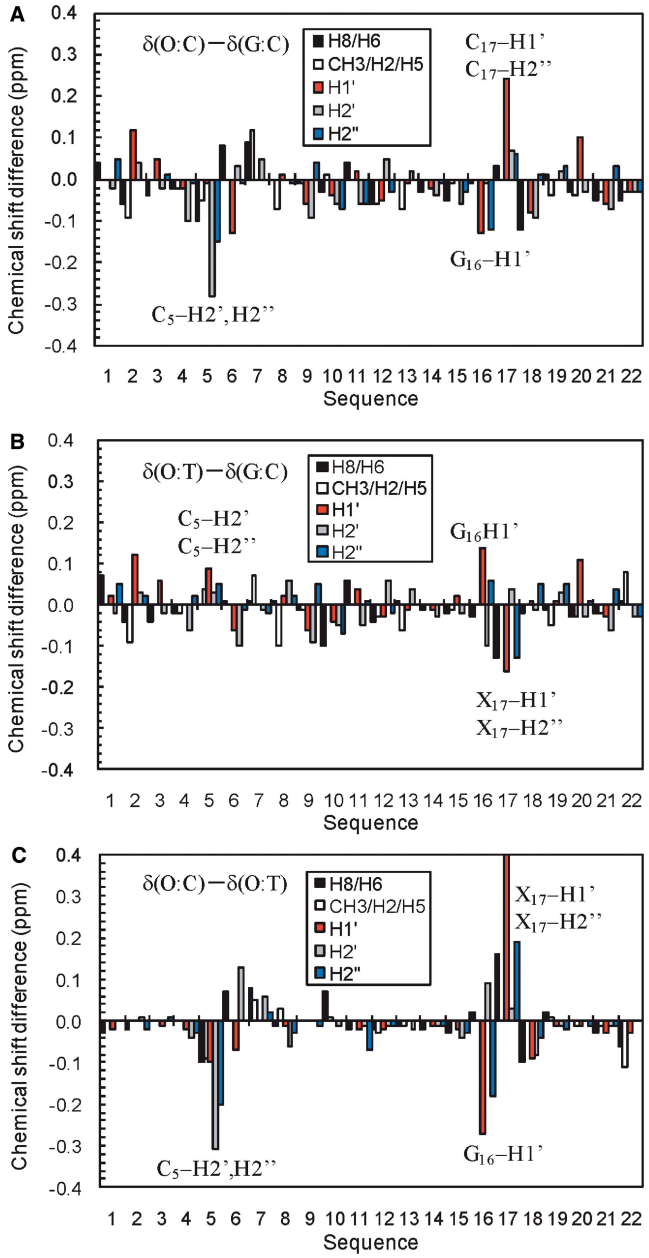

Figure 4. ^{1}H chemical shift differences between the DNA duplexes for H8/H6 (black), T CH_3/A H2/C H5 (white), H1′ (red), H2′ (gray), H2″ (blue): (**A**) δ(O:C duplex) – δ(G:C duplex), (**B**) δ(O:T duplex) – δ(G:C duplex), (**C**) δ(O:C duplex) – δ(O:T duplex). The protons which showed the large differences between the O:C and O:T duplexes are indicated by the names and sequential numbers.

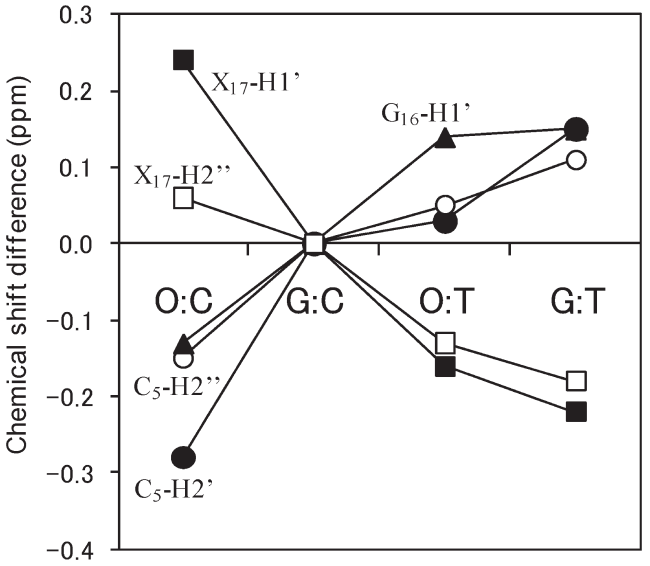

Figure 5. ^{1}H chemical shift deviations of the largely shifted protons of the mismatched DNA duplexes (O:C, O:T and G:T) from the G:C duplex. Those protons are indicated in the Figure 4: C_5-H2′ (closed circle), C_5-H2″ (open circle), G_{16}-H1′ (closed triangle), X_{17}-H1′ (closed square) and X_{17}-H2″ (open square) (X = C for O:C and X = T for O:T and G:T).

^{1}H NMR spectra. The duplex stability is also considered to be important for the estimation of mismatch DNA. Based on the temperature dependence of chemical shift change of isolated non-exchangeable proton resonances (A_4 H8, T_{15} H6), these isolated protons were cooperatively shifted with the temperature change, and the T_m values were determined. The T_m values for the O:C and O:T duplexes were 58 and 52°C, respectively, while those for the G:C and G:T duplexes were 63 and 57°C, respectively. The O:C duplex was less stable than the G:C duplex by 5°C, and as stable as the G:T duplex. The O:T duplex was less stable than the G:T duplex. The determined orders of T_m were G:C > O:C = G:T > O:T, which coincides with the previous report by using UV melting profile of Oxa mismatch DNAs (13). The base pair of O:C shows relatively high stability in DNA duplex compared with other base combinations. These results demonstrate that the introduction of the Oxa mismatch causes rather small change in the T_m values as previously reported (13).

We also observed the temperature dependence of the exchangeable proton resonances to obtain the information about the duplex stability and fluctuation. The imino protons at the terminal and penultimate base pairs disappeared ~10°C, and all the imino proton resonances disappeared <40°C, much lower than the T_m values, determined by the chemical shift change of the non-exchangeable protons, because the line broadening of the imino protons would depend on the fast exchange between the imino proton and water or the fluctuation of the base pairs. For the mismatch DNA duplexes (O:C, O:T, and G:T), unique temperature dependences of the exchangeable protons were observed in the temperature range between 5 and 30°C. The C_{17}-NH_{int} resonance of the O:C duplex was broader than those of C_5, C_7, C_9 and C_{20}, which are involved in the internal of the duplex. With elevating temperature, the C_{17}-NH_{int} resonance unchanged below 15°C, but with a further increase of the temperature, disappeared like the imino proton resonances of T_2 and T_{10} located in the peripheral of the duplex (Supplementary Figure S2). This exchange rate was considerably faster than those of the other G:C pairs, except for the terminal G:C pairs. Since the non-exchangeable protons involved in the mismatch pair did not show any

broadening in this temperature range, the broadening of the C_{17}-NH_{int} resonance would be caused by the exchange with bulk water. NMR spectrum of the O:T duplex at 5°C showed that the T_{17}-NH resonance at 9.21 ppm was as sharp as those of T_{15} and T_{19} involved in the center of the duplex. With temperature increasing from 5 to 25°C, the T_{17}-NH resonance became broad and completely disappeared ~30°C as well as the imino protons of T_2 and T_{10} located in the peripheral of the duplex. The exchange rate was faster than those of T_{15} and T_{19} involved in the A:T pairs (Supplementary Figure S2). The broadening of the T_{17}-NH proton would also be caused by the exchange with bulk water. The same phenomenon was observed for the imino protons of G_6 and T_{17} in the G:T duplex: The T_{17}-NH resonance of the G:T duplex was broadened and disappeared ~30°C, indicating that relatively rapid exchange of the imino protons with the solvent also occurs for the wobble pair of the G:T mismatch as well.

Characterization of the mismatch pair of O:C duplex

The chemical shift values (6.43 and 9.21 ppm) and its separation (2.78 ppm) of the C_{17}-NH_2 protons provide indications that the base pair of O_6:C_{17} is formed and stacked in the duplex. However, the downfield shift and broadness of the C_{17}-NH_2 protons suggest that the base pair does not take a Watson–Crick geometry, and a relatively rapid exchange occurs with water molecules. Similar results were reported for a 2-aminopruine(AP):cytosine mismatch in DNA duplex (34,35). The internal 4-amino proton in the AP:C mismatch of CAPC/GCG resonated at 8.94 ppm, and the resonance was broadened into the base line at 25°C but sharpen with decreasing temperature (34). They pointed that the C-NH_{int} proton resonance in the AP:C mismatch may shift to the further downfield than usual, due to an aromatic ring current shift, because the C-NH_{int} proton is likely to be 1.7–2.1 Å from the edge of the 2-AP base, and in a G:C pair, the C-NH_{int} proton is ~2.6 Å from the edge of the guanine base, leading to a smaller ring current shift. The AP:C mismatch pair was considered to take a wobble pair: The C-NH_{int} proton of AP:C is hydrogen bonded to the AP N1 atom, and the AP 2-amino group to the C N3 atom. The unusual downfield shift of the C_{17}-NH_{int} proton resonance may be caused by the short distance from the C_{17}-NH_{int} proton to the Oxa aromatic ring in the same wobble pair as the AP:C mismatch. According to previous theoretical calculation, oxanine and guanine show very similar electrostatic potential distribution on the aromatic plane (14), so the short distance to the aromatic ring could result in the more downfield shift. Strong NOE cross-peak of C_{17}-NH_{int} to O_6-NH_2 supports that the O:C base pair takes the wobble geometry similar to the AP:C mismatch, where the O_6-NH_2 proton resonance probably forms a hydrogen bond to the C_{17} N3 atom, and the C_{17}-NH_{int} and O_6-NH_2 protons are adjoining each other. The broadness of the O_6-NH_2 resonance also implies the hydrogen bond of O_6-NH_2 proton to the C_{17} N3 atom. In general, guanine and adenine amino groups often rotate at or near intermediate exchange on the NMR time scale, causing severe broadening of the amino proton resonances and making assignment of these protons difficult. The O_6-NH_2 resonance was broad, which were more likely to behave similarly to guanine and adenine amino protons involved in the hydrogen bond. The broad line shape of the C_{17}-NH_{int} proton resonance at 5°C and its disappearance with elevating the temperature suggest that the C_{17}-NH_{int} proton is likely located in the center of the wobble geometry, but no or very weak hydrogen bond is formed with the O_6 O1 atom. The pH dependence of the exchangeable protons of the O:C duplex showed the broadening of the C_{17}-NH_{int} proton resonance below pH 6 (data not shown). No resonance originated from the protonated cytosine hydrogen bonded to the Oxa moiety was observed at slightly acidic pH. The pH dependence of NMR spectra of the O:C duplex indicate that protonation of the C_{17} N3 position does not occur in the mismatch pair. These results of the pH titration also support the wobble geometry of the O:C mismatch.

In order to determine the geometry of the mismatch region, we focused on NOE cross-peaks from C_{17}-NH_{int} to G_{16}- and G_{18}-imino protons and to C_5- and C_7-NH_{int} protons. These NOE cross-peaks provide us with significant information for base pairing of O_6:C_{17} and its mutual position to the neighbor base pairs of C_5:G_{18} and C_7:G_{16}, although the NOEs are influenced by spin-diffusion effect and rapid exchange with water. The NOE cross-peaks from C_{17}-NH_{int} to G_{16}- and G_{18}-NH protons were observed, indicating the base pair formation and stacking of O_6:C_{17} in the duplex. However, no NOE cross-peak from C_{17}-NH_{int} to C_5-NH_{int} or C_7-NH_{int} proton was observed in the NOESY spectra even with a long mixing time (Figure 3A). Assuming that three consecutive base pairs of $C_5O_6C_7$/$G_{16}C_{17}G_{18}$ take a Watson–Crick geometry in regular B- or A-type DNA conformation, the NOE from C_{17}-NH_{int} to C_5-NH_{int} should be observable: in the regular B-type DNA, the distance from C_{17}-NH_{int} to C_5-NH_{int} is 2.9 Å, and that from C_{17}-NH_{int} to C_7-NH_{int} is >5 Å. On the other hand, in the regular A-type DNA conformation, the distances from C_{17}-NH_{int} to C_5-NH_{int} and to C_7-NH_{int} are comparable (3.5 Å). Judging from no NOE cross-peak between C_{17}-NH_{int} and C_5-NH_{int}, the base pair of O_6:C_{17} does not take a typical Watson–Crick geometry in the regular B-type DNA. Shortly afterward it will be discussed in detail on the basis of the determined structures.

Characterization of the mismatch pair of O:T duplex

There are two possibilities in the geometry of the O:T mismatch pair: a Watson–Crick geometry like G:C and a wobble geometry like G:T. In order to determine the geometry, NOE cross-peaks related to the imino proton of T_{17} (T_{17}-NH) were analyzed by NOESY spectra and compared between the O:T and G:T duplexes. The T_{17}-NH proton resonance of the O:T duplex was as sharp as that of the G:T duplex at 5°C, and resonated at 9.2 ppm. As compared to the chemical shift value of 11.62 ppm of the G:T duplex, the upfield shift by >2 ppm indicates that the T_{17}-NH proton of the O:T duplex is not involved in the hydrogen bond of the wobble geometry like G:T.

However, in terms of the NOE cross-peaks and their intensities involved in T_{17}-NH, the NOE pattern of the O:T duplex was almost identical to those of the G:T duplex, although those NOEs contain some spin diffusion effects because of the long mixing time (200 ms). In particular, the NOE intensity between O_6-NH_2 and T_{17}-NH of the O:T duplex was almost equal to that between G_6-NH_2 and T_{17}-NH of the G:T duplex. Both the NOEs were much weaker than that between G_6-NH_2 and G_6-NH of the G:T duplex. These NOEs indicate that, in the O:T mismatch pair, O_6-NH_2 and T_{17}-NH protons are not adjoining each other, denying the Watson–Crick geometry. The NOE cross-peaks from T_{17}-NH to G_{16}-NH, G_{18}-NH and to C_5-NH_{int} of the O:T and G:T duplexes (Figure 3B and C) exhibited the almost identical pattern with some spin diffusion effects. The conclusion that the O:T duplex takes an intermediate structure between the G:C and G:T duplexes is supported by following observation of the line width of the O_6-NH_2. The O_6-NH_2 resonance of the O:T duplex was much sharper than that of the O:C duplex, and was almost identical to that of the G:T duplex. As mentioned before, the line width of the G-NH_2 proton resonance involved in the hydrogen bond of the Watson–Crick pair is broad, because of its rotation at or near intermediate exchange on the NMR time scale. The G-NH_2 resonance of the G:T mismatch pair is known to be sharp, meaning the fast rotation of the amino group, because the G:T mismatch pair usually has two hydrogen bonds (N–H$\cdots$O = C) in the wobble base pair, where the G-NH_2 is not involved in the hydrogen bonds (6). Therefore, the sharpness of the O_6-NH_2 of the O:T duplex also suggests that the O_6-NH_2 protons are not involved in the strong hydrogen bond of the Watson–Crick pairing. Consequently, the O:T mismatch likely takes an intermediate base pairing between G:T (wobble) and G:C (Watson–Crick), and a hydrogen bond may exist between O_6-NH_2 and T_{17} O2 atom. The chemical shift deviations of the mismatch DNAs from the G:C duplex (Figure 5) agree with the intermediate structure of the O:T duplex.

Structure calculation and helical parameters

The investigation on the helical parameters provides us with the information about the local conformation of the O:C and O:T mismatches in detail. The rMD calculations were performed with the distance restraints derived from well-resolved NOE cross-peak intensities, and good convergence has been reached: The 17 final structures of the O:C duplex exhibited pairwise root-mean-squared deviation (RMSD) values of 0.81 ± 0.14 Å for all heavy atoms, and the O:T duplex exhibited the pairwise RMSD values of 0.85 ± 0.10 Å for all heavy atoms of the 15 final structures (Supplementary data). Energy terms of the final structures and the number of the NOE and dihedral violations were obtained and summarized in Table 1. These results indicate that all the distances were consistent with the final structures. The obtained structures of the O:C and O:T duplexes (Figure 6) were in the conformational range expected for B-form. The structural differences between the duplexes were small, and the prominent differences were observed around the mismatch pairs (Figure 7). Most of the conformational parameters calculated by Curves 5.3 are interrelated as shown previously (30,31). Selected helical parameters (shear, opening and helical twist) are given in Figure 8, and the complete list is given as Supplementary Figure S3. The shear parameter at the O_6:C_{17} pair reached a large positive value for the O:C duplex and a large negative value for the O:T duplex (Figure 8A), indicating that the bases in the base pair of O_6:C_{17} and the O_6:T_{17} moved oppositely. The helical twist showed symmetrical pattern at the base steps of 5 and 6 for the two duplexes (Figure 8C). The helical twists in the steps 5–6 and 6–7 were compensated each other. The common feature of the helical parameter of the two duplexes is large positive opening parameter (Figure 8B). The both base pairs of O_6:C_{17} and the O_6:T_{17} are opened toward major groove, as compared with typical Watson–Crick geometry.

The obtained structures of the O:T duplex showed that the distance between T_{17}-NH and O_6 O6 atom was 2.21 ± 0.13 Å (Figure 9), suggesting that a weak hydrogen bond exists between them. On the other hand, for the O:C duplex, the distance between C_{17}-NH_{int} and O_6 O6 atoms was 3.39 ± 0.19 Å, indicating that there is no direct hydrogen bond between them. The obtained structures of the O:C duplex showed rather short distance ($d < 3.0$ Å) between C_{17}-NH_{int} and C_5-NH_{int} which did not show any NOE cross-peak (Figure 3A). It was reported for C:T mismatch pairs that exchangeable protons involved in the hydrogen bond via water

Table 1. NMR constraints and structural statistics for the O:C and O:T duplexes

	O:C duplex	O:T duplex
NMR constraints		
Distance constraints	231	225
Intraresidue	141	150
Interresidue	90	75
Dihedral angles	102	102
Hydrogen bonds	62	62
Structural statistics for final structures (kcal/mol)		
E_{total}	297 ± 11	281 ± 13
E_{bond}	36 ± 1	36 ± 1
E_{angle}	370 ± 3	342 ± 2
$E_{improper}$	60 ± 1	60 ± 1
E_{vdw}	-309 ± 3	-311 ± 3
E_{noe}	17 ± 1	12 ± 1
E_{cdih}	0 ± 0	0 ± 0
RMSD from idealized geometry		
Bond length (Å)	0.007 ± 0	0.007 ± 0
Bond angle (°)	1.34 ± 0.004	1.29 ± 0.003
Impropers (°)	0.9 ± 0.003	0.9 ± 0.004
Number of NOE violations		
$d > 0.25$ Å	0	0
$0.25 > d > 0.15$ Å	7	4
RMSD of violation (Å)	0.05 ± 0.001	0.04 ± 0.002
Dihedral violation		
Number of violation (>5°)	0	0
Pairwise RMSD for all heavy atoms (Å)	0.81 ± 0.14	0.85 ± 0.10

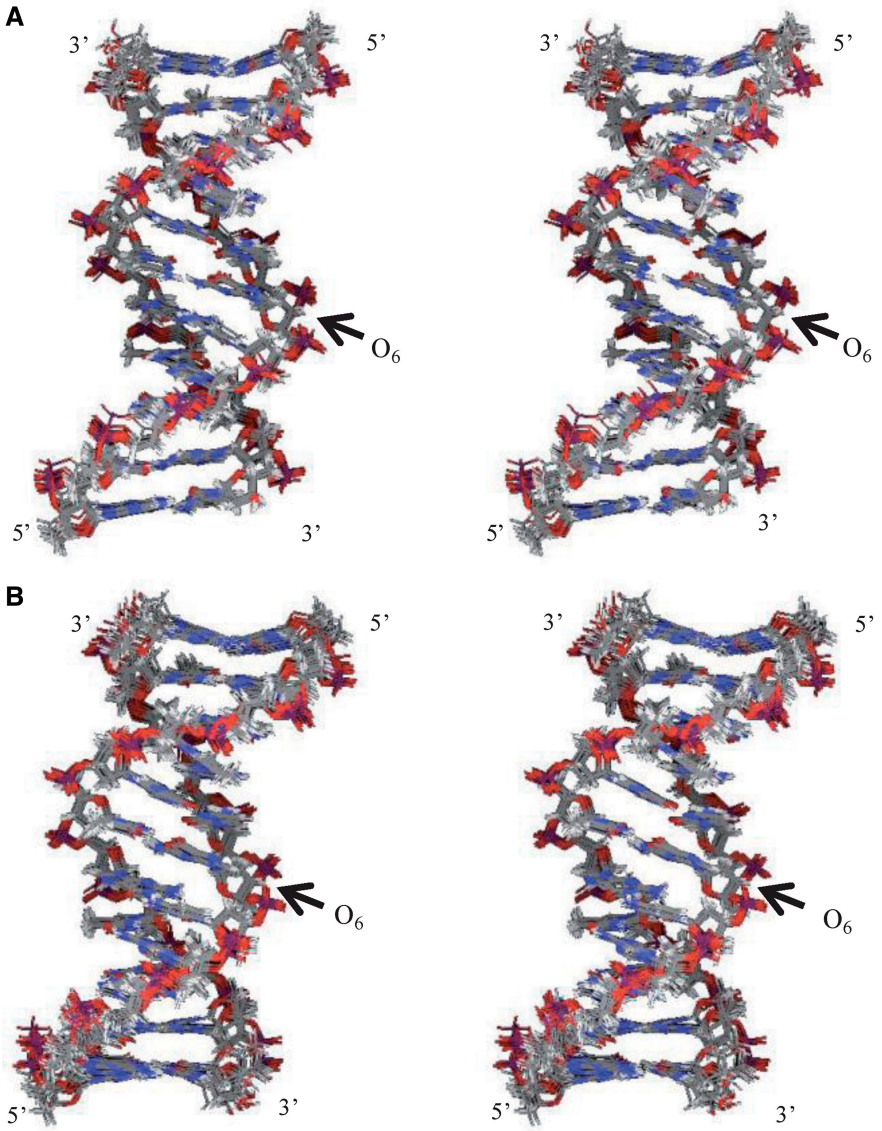

Figure 6. Superposition of overlapped final structures of (**A**) O:C duplex and (**B**) O:T duplex. View of the major groove of the superposition of the heavy atoms of the duplexes. The O_6 position is indicated by an arrow.

molecule did not show any observable NOEs (36,37). Since the line width of C_{17}-NH_{int} was broad and it disappeared with elevating the temperature as above mentioned, no NOE cross-peak between C_{17}-NH_{int} and C_5-NH_{int} is probably caused by the rapid exchange of the amino protons with water. Taking account of the chemical shift values (6.43 and 9.21 ppm), its separation (2.78 ppm), the broad line width of the C_{17}-NH_2 protons, and rather high melting temperature of the O:C duplex, there may be a hydrogen bond from the C_{17}-NH_{int} to O_6 O6 atom (d = 3.4 Å) via water molecule (Figure 9). Since such a water molecule involved in the hydrogen bond is known to make the exchangeable NH proton, such as imino and amino proton, exchange faster with water (36–38), the proximity of C_{17}- and C_5-NH_{int} to the water molecule hydrogen bonded to the O_6 O6 atom may contribute to diminishing the NOE cross-peak.

The angle formed by the purine N9 or pyrimidine N1 and C1′-C1′ intrabase pair vector defines λ. Each base pair may be characterized by two λ values, relating to each strand of the duplex (5,8). The values of λ_1 and λ_2 (the subscript 1 corresponds to residues 1–11 and 2 designates residues 12–22) were determined for the O:C and O:T duplexes. For all the base pairs except the O:C and O:T mismatch pairs, a high degree of symmetry was observed in the λ_1 and λ_2 values in the range of 51–57°. However, the O:C mismatch pair showed asymmetry of the λ_1 (67.4° ± 1.1°) and λ_2 (55.4° ± 1.6°) values, and for the O:T mismatch pair, the values of λ_1 and λ_2 were 50.0 ± 1.0° and 68.8 ± 0.6°, respectively. In B-DNA containing a G:T mismatched base pair, the values of λ_1 and λ_2 were reported to be ~40° and 70°, respectively (5,8). The λ_2 value of the O:T mismatch pair is as large as that of the reported G:T wobble pair, although its λ_1 value is in

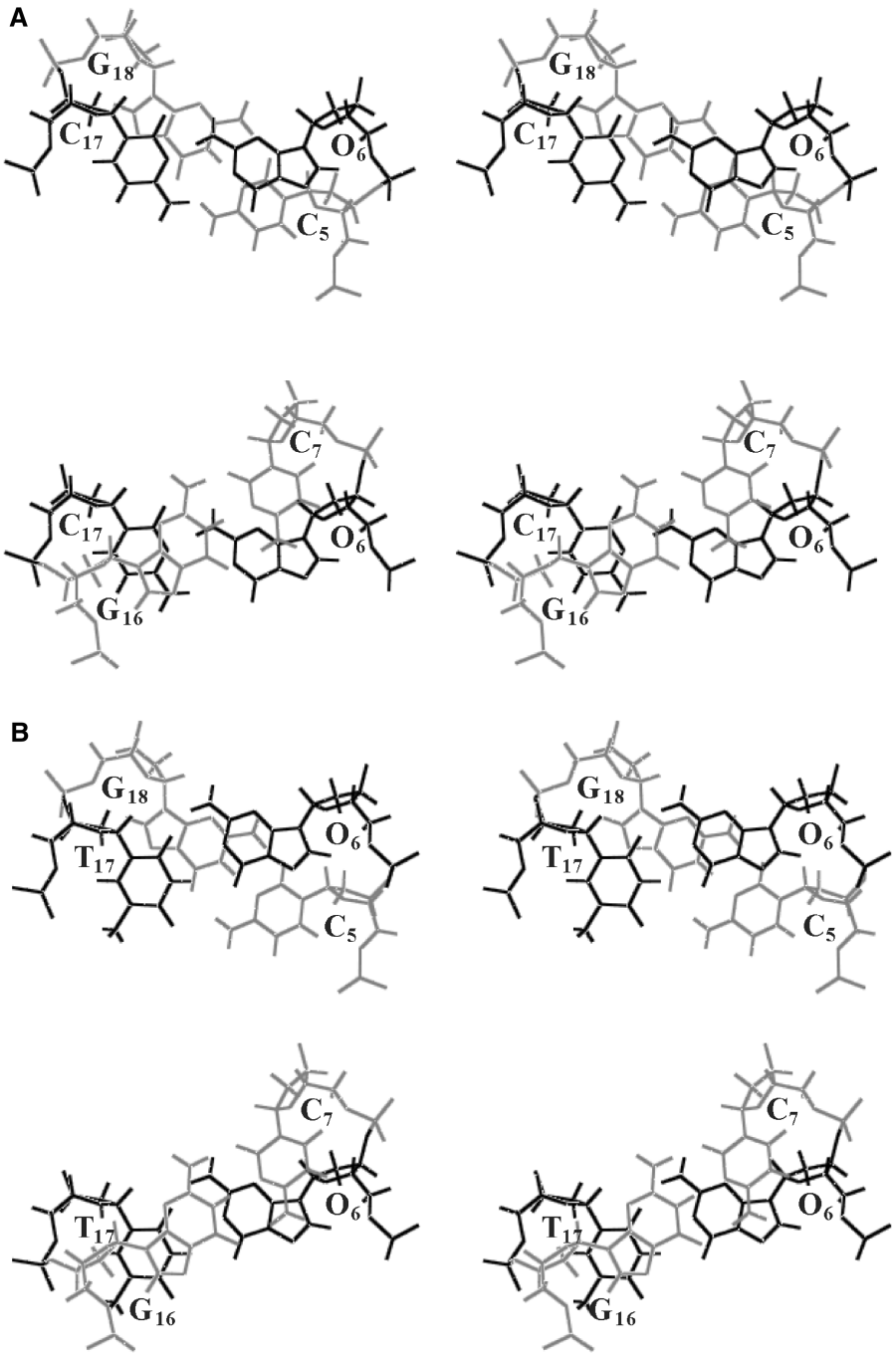

Figure 7. Base stacking interaction of (**A**) $C_5\underline{O_6}/\underline{C_{17}}G_{18}$ and $\underline{O_6}C_7/G_{16}\underline{C_{17}}$ in the O:C duplex, and (**B**) $C_5\underline{O_6}/\underline{T_{17}}G_{18}$ and $\underline{O_6}C_7/G_{16}\underline{T_{17}}$ in the O:T duplex. The mismatch pairs of O_6:C_{17} and O_6:T_{17} are shown in dark, and the canonical G:C pairs in light.

the range expected for the Watson–Crick pair. On the other hand, the λ_1 and λ_2 values of the O:C duplex are reversed; the large λ_1 like λ_2 of G:T, and the moderate λ_2 in the range expected for the Watson–Crick pair.

DISCUSSION

We have presented that the DNA duplexes containing one dOxa residue take two kinds of wobble geometries, depending on the opposite bases (Figure 9). The two wobble geometries are characterized by the mutual position of the Oxa moiety to the pyrimidine base (C or T) in the counter strand. The O:C duplex exhibits that the Oxa moiety shifted toward the major groove and the paired cytosine of C_{17} shifted toward the minor groove, where the O_6-NH_2 is hydrogen bonded to the C_{17}-N3 atom. On the other hand, the O:T duplex exhibits that the Oxa moiety shifted toward the minor groove and the paired T_{17} shifted toward the major groove, where the internal proton of O_6-NH_2 is partially hydrogen bonded

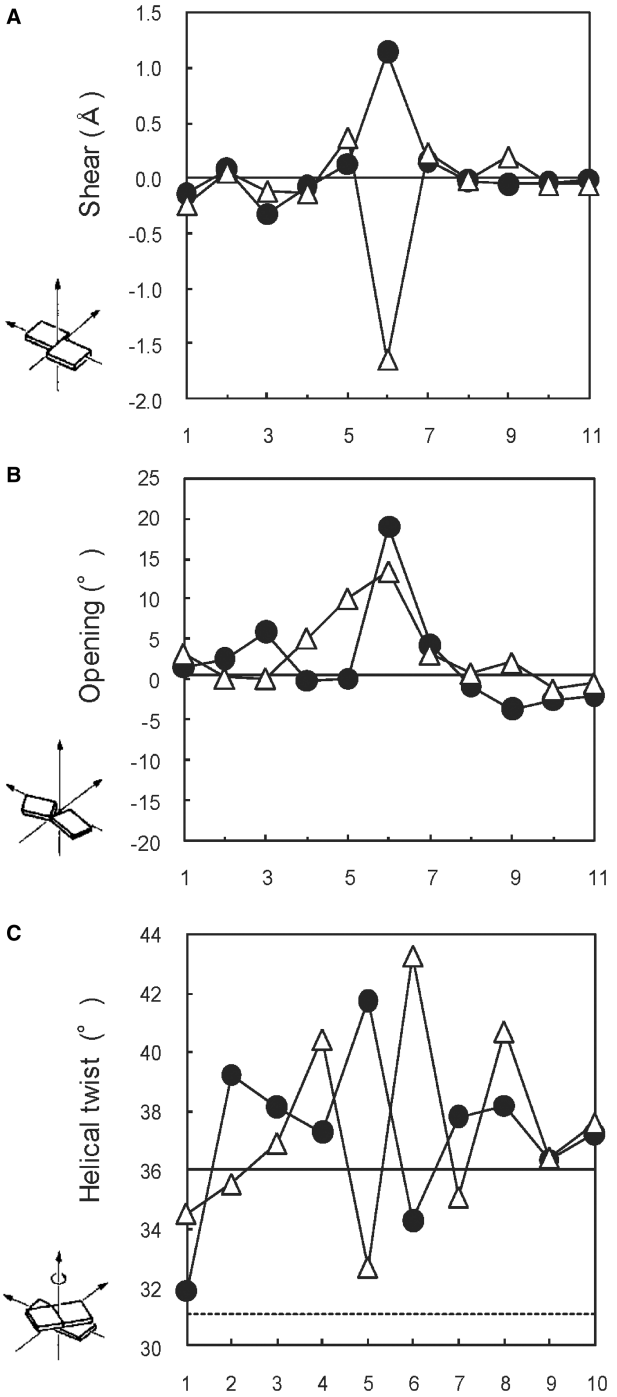

Figure 8. Helical parameters (**A**) shear, (**B**) opening and (**C**) helical twist of the O:C and O:T duplexes. Open triangles and closed circles indicate the O:C and O:T duplex, respectively.

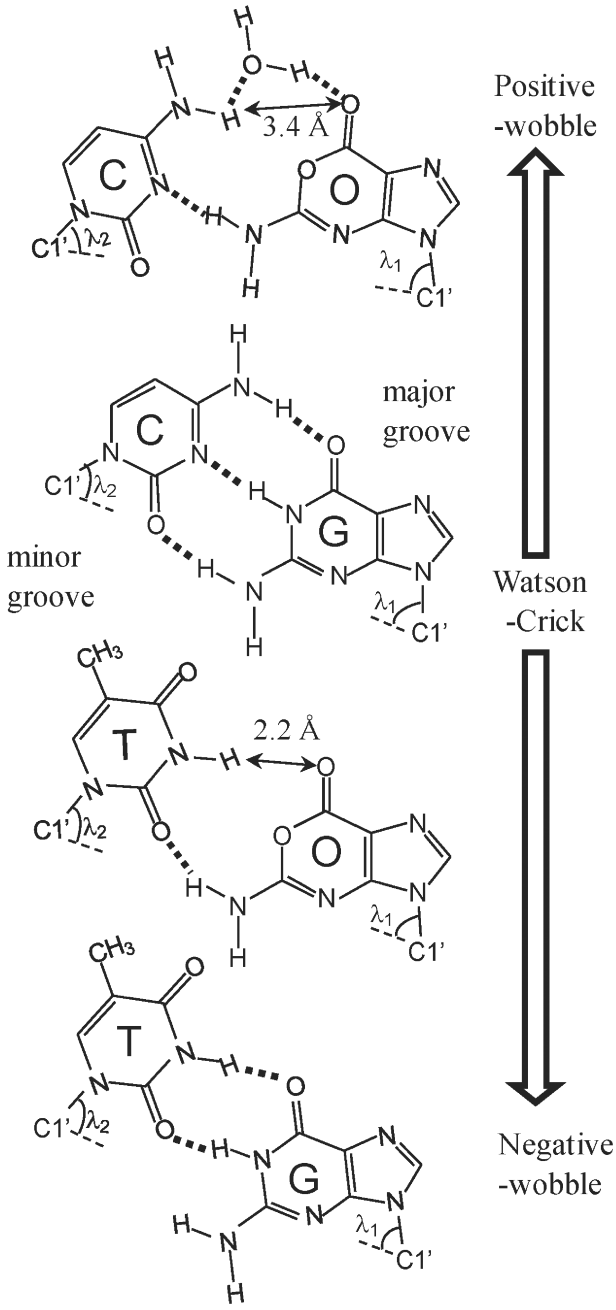

Figure 9. Possible base pairings of the O:C, O:T, G:C and G:T pairs with expected hydrogen bonds.

to the T_{17}-O2 atom. The obtained geometries of the O:C and O:T mismatches fairly coincide with those derived from theoretical MD calculations of the duplex DNA with O:C and O:T pairs (14). The relative position and the direction of the displacement of the pyrimidine:purine pair in the present study agreed with those in the theoretical calculation. In terms of the helical parameters, the most prominent change exists in the value of shear parameter. The shear value is around zero in Watson–Crick geometry, where imino protons of G and T are hydrogen bonded to C N3 and A N1 atoms, respectively. The shear values of the O:C and O:T duplexes were positive and negative, respectively, so hereafter, we call the wobble geometry with the positive shear value, 'positive-wobble' geometry, and that with the negative shear, 'negative-wobble' geometry. The negative-wobble geometries have been reported for many mismatch pairs, such as G:T and A:C (or A^+:C). In particular, the G:T mismatch has been

studied extensively and shown to take the negative-wobble geometry (7,39). Previous studies of A:C mismatch pair in DNA suggested that the A:C mismatch also existed in the negative-wobble geometry, in which the exocyclic amino group of mispaired Ade hydrogen bonded with Cyt N3 imino nitrogen (1–4). In the negative-wobble geometries of the G:T and C:A mismatch pairs, the purine base projects in the minor groove and pyrimidine into the major groove. The characteristics of the negative-wobble geometry are a rather short distance between the C1′ protons of the mismatch pair and a large difference between the bond angles (λ_1 and λ_2) of the pyrimidine and purine residues (8). NMR spectra of the negative-wobble geometry of typical G:T in the B-DNA duplex are characterized by two hydrogen bonds where the G-NH resonates at 10–11 ppm and T-NH at 11–12 ppm (5,32,33). In the case of partially distorted G:T mismatch where the G-NH and G-NH_2 are hydrogen bonded to T O2 atom, the T-NH proton resonance was shifted to the upfield in the range of 9–10 ppm (40). According to the chemical shift value (9.2 ppm) of the T_{17}-NH proton of the O:T duplex, the O:T mismatch pair takes an intermediate geometry between the negative-wobble and Watson–Crick geometries. Recently, non-hydrogen bonding guanine–difluorotoluene (G:F) pair was reported to take also an intermediate geometry between the negative-wobble of G:T and the Watson–Crick geometries (41). The G:F mismatch pair stacks relatively well into the helix without any hydrogen bond between the mismatch pair, suggesting that the intermediate geometry is likely stabilized by the base stacking.

On the other hand, the O:C mismatch pair takes the positive-wobble geometry differing in the mutual geometry of the purine:pyrimidine pair from the G:T and A:C mismatch pairs. Not many positive-wobble geometries of mismatch DNA have been reported, and it is remarkable that in the AP:C mismatch in DNA duplex, the purine 2-amino group is hydrogen bonded to the pyrmidine N3 (34,35). In the positive-wobble geometry of the O:C mismatch, the O_6-NH_2 group is hydrogen bonded to the C_{17} N3 atom. Addition to the chemical shift values and the relatively rapid exchange of the C_{17}-NH_{int} protons of the O:C duplex, its unusual NOE pattern around the C_{17}-NH_{int} proton indicate that the O:C mismatch pair takes the positive-wobble geometry but not Watson–Crick geometry, and that the expected hydrogen bond between O_6 O1 and C_{17}-NH_{int} should be weak or could not be formed. It is possibly because the O1 atom of Oxa has an sp^3 hybrid orbital and the lone pairs of electrons exist out of the plane. Detailed NOE analyses revealed that there are some differences in the positive-wobble geometries between the O:C and AP:C duplexes. In the AP:C wobble pair of $C_4\underline{AP}_5C_6/G_{13}\underline{C}_{14}G_{15}$, the C_{14}-NH_{int} proton was hydrogen bonded to the AP_5 N1 atom, and showed NOE cross-peaks with the C_4-NH_2 protons (34). As mentioned in the 'Results' section, the NOE pattern in the region of $C_5\underline{O}_6C_7/G_{16}\underline{C}_{17}G_{18}$ was different from that of the typical B-DNA and the base pair dynamics of the O:C was also changed. The O:C mismatch pair takes an intermediate geometry between positive-wobble (AP:C) and Watson–Crick (G:C) geometries, and the C_{17}-NH_{int} proton is likely hydrogen bonded to O_6 O6 atom of oxanine moiety via water molecule. As U:C mismatch pair which form only a single base–base hydrogen bond are stabilized by a water molecule, which bridges between the ring nitrogens (42), the hydrogen bond via the water molecule probably contributes to the high thermodynamic stability of the O:C duplex. The mismatch pair of the O:C duplex should be more locally fluctuated, as compared with that of the AP:C duplex. Consequently, the difference between the two mismatch duplexes is not only the geometry but the base pair dynamics. It was reported for the AP:C mismatch pair that protonation of the mismatched AP N1 or C N3 positions allowed formation of a second hydrogen bond and stabilization of the AP:C pair, and that the stability of the AP:C mismatch was dependent upon pH (34,35). The protonation of C_{17} in the O:C mismatch was not observed, possibly because the hydrogen bond of protonated cytosine to the oxanine O1 does not stabilize the duplex structure due to the sp^3 hybrid orbital of the O1 atom.

G:T mismatch pair is among the most commonly observed mismatches in genomic DNA (43). It might be expected that the more stable the mismatch, the less efficient is its repair. However, the stable G:T mismatch is among the most efficiently repaired mismatches in DNA, which may suggest that its repair is based on recognition of structure (44–46). While thermodynamics may play a major role in the frequency of the occurrences of different mismatches, it is more likely that the enzymatic recognition and repair of mismatches are influenced by the geometry and 3D structure of the mismatch (7,8,47,48). Repair enzymes that recognize and excise G:T mismatches may recognize subtle backbone perturbations such as in the torsion angle perturbations or the base pair parameters (5). It has been proposed that mismatch repair enzymes may directly recognize the base pair parameters λ_1 and λ_2, which are approximately the same in canonical G:C and A:T pairs but are highly asymmetric for G:T mismatches ($\lambda_1 = 40^\circ$ and $\lambda_2 = 70^\circ$) (5,8). In the present study, the positive-wobble geometry of the O:C mismatch showed the large λ_1 value (67.4°) of the O_6 purine base, indicating that the O:C wobble geometry is reversely asymmetric, as compared with the G:T mismatch. The negative-wobble geometry of the O:T mismatch showed the large λ_2 value (68.8°) of the T_{17} pyrimidine base, but the moderate λ_1 value (50.0°) of the O_6 base. Similar tendency of the λ values was reported for the non-hydrogen bonding G:F pair ($\lambda_1 = 53.5^\circ$ and $\lambda_2 = 70.0^\circ$) (41), indicating that the Oxa mismatch pairs with no hydrogen bond to the O1 position of the Oxa base can be wobbled widely, and may occupy some positions in the double strands that optimize the stacking with adjacent bases. The asymmetric patterns of the λ_1 and λ_2 values of the O:C and O:T duplexes may be one of the reasons for not recognized by the G:T mismatch repairing enzyme.

The determined structures exhibit that the wobble geometries of the O:C and O:T mismatches make some influence on only neighboring base pairs in the helical parameters, such as helical twist. Aside from the lesion site, the duplex structure, including the flanking base pair, are not highly perturbed by the presence of the

lesion. In the previous studies of the mismatches of G:T, G:A and A:C, the perturbations caused by the mismatches also extend only to its neighboring Watson–Crick base pair, thus providing a structural basis for the applicability of the nearest-neighbor model to the thermodynamics of internal mismatches (5,49,50). The flanking wobble base pairs of O:C and O:T seem quite stable in terms of the thermodynamic property, and do not perturb the cooperative feature of the duplex stability, so that the nearest-neighbor model could also be applicable to the mismatch containing Oxa. The large increases in the exchange rate of the exchangeable protons in the mismatch pairs with water indicate that the local base pair fluctuations exist in the mismatches of the O:C and O:T, and the fluctuations may be as large as those at the terminus of the duplex. Previous theoretical calculation (14) indicates that the G:C → O:C substitution reduces the stability of the duplex, but probably less than would be expected from the existence of repulsive interactions in the O:C dimer between oxanine O1 and cytosine N3 atoms, and that the G:C → O:C mutation was expected to increase the flexibility of the hydrogen bonded dimer, which fluctuates between binding modes. Oxa forms relatively stable base pairing with C compared with other matches with T, G and A. The O:C mismatch would maintain thermodynamically stable interaction without severe influence on the local structure of DNA duplex, but from a dynamic point of view, the mismatch pair has been largely changed by the substitution of Oxa with G. Similar local fluctuations in the base pairing were reported for DNA duplex containing 6-thioguanine (51,52). They pointed that the fast exchange of the imino proton with water may be caused by a faster apparent opening rate. The base pairing geometry of Oxa to C or T could largely change between the positive- and negative-wobble geometries, and the formed mismatched base pairs themselves are fluctuating. In the case of the base excision repair (BER) system, bacterial AlkA (3-methyladenine DNA glycosylase II) and endonuclease VIII was found to possess repair activities on Oxa in oligodeoxynucleotides (53). Cao and co-workers (15,54) also reported that bacterial endonuclease V and human AAG alkyladenine glycosylase shows BER activity on Oxa. The uniqueness of the Oxa base paring may be one of the reasons for the difficulties in finding the specific repairing enzyme for Oxa. In addition, Oxa mediates a novel genotoxic mechanism related to the formation of DNA–protein cross-link (DPC) (55). It was demonstrated that in the case of Oxa-related genotoxicity (Oxa-mediated DPC formation and its relevant events), the nucleotide excision and recombination repair system would play a more efficient role than BER system (56). The structures solved in this work indicate that the presence of the O:C or O:T mismatches causes the localized distortion and fluctuation of the DNA duplexes. The fluctuation of the O:C or O:T base pair may possibly cause the reaction of DPC, leading to the cytotoxity. The static structure and local fluctuation of the O:C and O:T base pair would be related to the recognition and repair of Oxa mismatch sites in DNA.

SUPPLEMENTARY DATA

Supplementary Data are available at NAR Online: Supplementary Tables 1–4, Supplementary Figures 1–3.

ACKNOWLEDGEMENTS

We thank Ms Sachiko Dairaku for her assistance with measuring NMR spectra.

FUNDING

Grant-in-Aid for Scientific Research from the Ministry of Education, Science, Sports, and Culture (17570092 to K.K.); Basic Science Research Program through the National Research Foundation of Korea (NRF) funded by the Ministry of Education, Science and Technology (2010-0010110 to S.P.P.). This work was partly performed in Nanotechnology Support Project in Central Japan (Institute for Molecular Science), financially supported by Nanotechnology Network of the Ministry of Education, Culture, Sports, Science and Technology (MEXT), Japan. Funding for open access charge: Grant-in-Aid for Scientific Research from the Ministry of Education, Science, Sports, and Culture.

Conflict of interest statement. None declared.

REFERENCES

1. Hunter,W.N., Brown,T., Anand,N.N. and Kennard,O. (1986) Structure of an adenine-cytosine base pair in DNA and its implications for mismatch repair. *Nature*, **320**, 552–555.
2. Gao,X.L. and Patel,D.J. (1987) NMR studies of A•C mismatches in DNA dodecanucleotides at acidic pH. Wobble A(*anti*).C(*anti*) pair formation. *J. Biol. Chem.*, **262**, 16973–16984.
3. Patel,D.J., Kozlowski,S.A., Ikuta,S. and Itakura,K. (1984) Deoxyadenosine•deoxycytidine pairing in the d(C-G-C-G-A-A-T-T-C-A-C-G) duplex: conformation and dynamics at and adjacent to the dA•dC mismatch site. *Biochemistry*, **23**, 3218–3226.
4. Sarma,M.H., Gupta,G., Sarma,R.H., Bald,R., Engelke,U., Oei,S.L., Gessner,R. and Erdmann,V.A. (1987) DNA structure in which an adenine-cytosine mismatch pair forms an integral part of the double helix. *Biochemistry*, **26**, 7707–7715.
5. Allawi,H.T. and SantaLucia,J. Jr (1998) NMR solution structure of a DNA dodecamer containing single G•T mismatches. *Nucleic Acids Res.*, **26**, 4925–4934.
6. Allawi,H.T. and SantaLucia,J. Jr (1997) Thermodynamics and NMR of internal G•T mismatches in DNA. *Biochemistry*, **36**, 10581–10594.
7. Hunter,W.N., Brown,T., Kneale,G., Anand,N.N., Rabinovich,D. and Kennard,O. (1987) The structure of guanosine-thymidine mismatches in B-DNA at 2.5-Å resolution. *J. Biol. Chem.*, **262**, 9962–9970.
8. Goodman,M.F. (1997) Hydrogen bonding revisited: geometric selection as a principal determinant of DNA replication fidelity. *Proc. Natl Acad. Sci. USA*, **94**, 10493–10495.
9. Shimada,N., Yagisawa,N., Naganawa,H., Takita,T., Hamada,M., Takeuchi,T. and Umezawa,H. (1981) Oxanosine, a novel nucleoside from actinomycetes. *J. Antibiot.*, **34**, 1216–1218.
10. Suzuki,T., Yamaoka,R., Nishi,M., Ide,H. and Makino,K. (1996) Isolation and characterization of a novel product, 2′-deoxyoxanosine, from 2′-deoxyguanosine, oligonucleotide, and calf thymus DNA treated by nitrous acid and nitric oxide. *J. Am. Chem. Soc.*, **118**, 2515–2516.
11. Suzuki,T., Matsumura,Y., Ide,H., Kanaori,K., Tajima,K. and Makino,K. (1997) Deglycosylation susceptibility and base-pairing

stability of 2′-deoxyoxanosine in oligodeoxynucleotide. *Biochemistry*, **36**, 8013–8019.
12. Suzuki,T., Ide,H., Yamada,M., Endo,N., Kanaori,K., Tajima,K., Morii,T. and Makino,K. (2000) Formation of 2′-deoxyoxanosine from 2′-deoxyguanosine and nitrous acid: mechanism and intermediates. *Nucleic Acids Res.*, **28**, 544–551.
13. Pack,S.P., Nonogawa,M., Kodaki,T. and Makino,K. (2005) Chemical synthesis and thermodynamic characterization of oxanine-containing oligodeoxynucleotides. *Nucleic Acids Res.*, **33**, 5771–5780.
14. Hernández,B., Soliva,R., Luque,F.J. and Orozco,M. (2000) Misincorporation of 2′-deoxyoxanosine into DNA: a molecular basis for NO-induced mutagenesis derived from theoretical calculations. *Nucleic Acids Res.*, **28**, 4873–4883.
15. Hitchcock,T.M., Gao,H. and Cao,W. (2004) Cleavage of deoxyoxanosine-containing oligodeoxyribonucleotides by bacterial endonuclease V. *Nucleic Acids Res.*, **32**, 4071–4080.
16. Pack,S.P. and Makino,K. (2010) Synthesis of 2′-deoxyoxanosine from 2′-deoxyguanosine, conversion to its phosphoramidite, and incorporation into oxanine-containing oligodeoxynucleotides. *Curr. Protoc. Nucleic Acid Chem.*, Chapter 4, Unit 4 39.
17. Pack,S.P., Doi,A., Choi,Y.S., Kim,H.B. and Makino,K. (2010) Accurate guanine:cytosine discrimination in T4 DNA ligase-based single nucleotide polymorphism analysis using an oxanine-containing ligation fragment. *Anal. Biochem.*, **398**, 257–259.
18. Pack,S.P., Doi,A., Choi,Y.S., Kodaki,T. and Makino,K. (2010) Biomolecular response of oxanine in DNA strands to T4 polynucleotide kinase, T4 DNA ligase, and restriction enzymes. *Biochem. Biophys. Res. Commun.*, **391**, 118–122.
19. Wüthrich,K. (1986) *NMR of Proteins and Nucleic Acids*. Wiley-Interscience, New York.
20. Piantini,U., Sørensen,O.W. and Ernst,R.R. (1982) Multiple quantum filters for elucidating NMR coupling networks. *J. Am. Chem. Soc.*, **104**, 6800–6801.
21. Davis,D.G. and Bax,A. (1985) Assignment of complex proton NMR spectra via two-dimensional homonuclear Hartmann-Hahn spectroscopy. *J. Am. Chem. Soc.*, **107**, 2820–2821.
22. Bax,A. and Davis,D.G. (1985) MLEV-17-based two-dimensional homonuclear magnetization transfer spectroscopy. *J. Magn. Reson.*, **65**, 355–360.
23. Jeener,J., Meier,B.H., Bachmann,P. and Ernst,R.R. (1979) Investigation of exchange processes by two-dimensional NMR spectroscopy. *J. Chem. Phys.*, **71**, 4546–4553.
24. Williamson,J.R. and Boxer,S.G. (1989) Multinuclear NMR studies of DNA hairpins. 1. Structure and dynamics of d(CGCGTTGTT CGCG). *Biochemistry*, **28**, 2819–2831.
25. Piotto,M., Saudek,V. and Sklenar,V. (1992) Gradient-tailored excitation for single-quantum NMR spectroscopy of aqueous solutions. *J. Biomol. NMR*, **2**, 661–665.
26. Brünger,A.T. (1993) *X-PLOR Version 3.1: A System for X-ray Crystallography and NMR*. Yale University Press, New Haven.
27. Kuszewski,J., Schwieters,C. and Clore,G.M. (2001) Improving the accuracy of NMR structures of DNA by means of a database potential of mean force describing base-base positional interactions. *J. Am. Chem. Soc.*, **123**, 3903–3918.
28. Mujeeb,A., Kerwin,S.M., Kenyon,G.L. and James,T.L. (1993) Solution structure of a conserved DNA sequence from the HIV-1 genome: Restrained molecular dynamics simulation with distance and torsion angle restraints derived from two-dimensional NMR spectra. *Biochemistry*, **32**, 13419–13431.
29. Kanaori,K., Tamura,Y., Wada,T., Nishi,M., Kanehara,H., Morii,T., Tajima,K. and Makino,K. (1999) Structure and stability of the consecutive stereoregulated chiral phosphorothioate DNA duplex. *Biochemistry*, **38**, 16058–16066.
30. Lavery,R. and Sklenar,H. (1989) Defining the structure of irregular nucleic acids: conventions and principles. *J. Biomol. Struct. Dyn.*, **6**, 655–667.
31. Lavery,R. and Sklenar,H. (1988) The definition of generalized helicoidal parameters and of axis curvature for irregular nucleic acids. *J. Biomol. Struct. Dyn.*, **6**, 63–91.
32. Kalnik,M.W., Kouchankdjian,M., Li,B.F., Swann,P.F. and Patel,D.J. (1988) Base pair mismatches and carcinogen-modified bases in DNA: an NMR study of G•T and G•O4meT pairing in dodecanucleotide duplexes. *Biochemistry*, **27**, 108–115.
33. Hare,D., Shapiro,L. and Patel,D.J. (1986) Wobble dG•dT pairing in right-handed DNA: solution conformation of the d(C-G-T-G-A-A-T-T-C-G-C-G) duplex deduced from distance geometry analysis of nuclear Overhauser effect spectra. *Biochemistry*, **25**, 7445–7456.
34. Fagan,P.A., Fabrega,C., Eritja,R., Goodman,M.F. and Wemmer,D.E. (1996) NMR study of the conformation of the 2-aminopurine:cytosine mismatch in DNA. *Biochemistry*, **35**, 4026–4033.
35. Sowers,L.C., Boulard,Y. and Fazakerley,G.V. (2000) Multiple structures for the 2-aminopurine-cytosine mispair. *Biochemistry*, **39**, 7613–7620.
36. Boulard,Y., Cognet,J.A. and Fazakerley,G.V. (1997) Solution structure as a function of pH of two central mismatches, C. T and C. C, in the 29 to 39 K-ras gene sequence, by nuclear magnetic resonance and molecular dynamics. *J. Mol. Biol.*, **268**, 331–347.
37. Allawi,H.T. and SantaLucia,J. Jr (1998) Thermodynamics of internal C•T mismatches in DNA. *Nucleic Acids Res.*, **26**, 2694–2701.
38. Bhaumik,S.R., Chary,K.V., Govil,G., Liu,K. and Miles,H.T. (1997) Homopurine and homopyrimidine strands complementary in parallel orientation form an antiparallel duplex at neutral pH with A-C, G-T, and T-C mismatched base pairs. *Biopolymers*, **41**, 773–784.
39. Allawi,T.H. and SantaLucia,J.J. (1998) NMR solution structure of a DNA dodecamer containing single G-T mismatches. *Nucleic Acids Res.*, **26**, 4925–4934.
40. Chin,K.H., Chen,F.M. and Chou,S.H. (2003) Solution structure of the ActD-5'-CCGTT3GTGG-3' complex: drug interaction with tandem G•T mismatches and hairpin loop backbone. *Nucleic Acids Res.*, **31**, 2622–2629.
41. Pfaff,D.A., Clarke,K.M., Parr,T.A., Cole,J.M., Geierstanger,B.H., Tahmassebi,D.C. and Dwyer,T.J. (2008) Solution structure of a DNA duplex containing a guanine-difluorotoluene pair: A wobble pair without hydrogen bonding? *J. Am. Chem. Soc.*, **130**, 4869–4878.
42. Holbrook,S.R., Cheong,C., Tinoco,I.J. and Kim,S.H. (1991) Crystal structure of an RNA double helix incorporating a track of non-Watson-Crick base pairs. *Nature*, **353**, 579–581.
43. Sloane,D.L., Goodman,M.F. and Echols,H. (1998) The fidelity of base selection by the polymerase subunit of DNA polymerase III holoenzyme. *Nucleic Acid Res.*, **16**, 6465–6475.
44. Modrich,P. (1987) DNA mismatch correction. *Annu. Rev. Biochem.*, **56**, 435–466.
45. Kramer,B., Kramer,W. and Fritz,H.-J. (1984) Different base/base mismatches are corrected with different efficiencies by the methyl-directed DNA mismatch-repair system of *E. coli*. *Cell*, **38**, 879–887.
46. Dohet,C., Wagner,R. and Radman,M. (1985) Repair of defined single base-pair mismatches in Escherichia coli. *Proc. Natl Acad. Sci. USA*, **82**, 503–505.
47. Moran,S., Ren,R.X., Sheils,C.J., Rumney,S. and Kool,E.T. (1996) Non-hydrogen bonding 'terminator' nucleosides increase the 3′-end homogeneity of enzymatic RNA and DNA synthesis. *Nucleic Acid Res.*, **24**, 2044–2052.
48. Hunter,W.N. (1992) Crystallographic studies of DNA containing mismatches, modified and unpaired bases. *Methods Enzymol.*, **211**, 221–231.
49. Allawi,H.T. and SantaLucia,J. Jr (1998) Nearest neighbor thermodynamic parameters for internal G•A mismatches in DNA. *Biochemistry*, **37**, 2170–2179.
50. Allawi,H.T. and SantaLucia,J. Jr (1998) Nearest-neighbor thermodynamics of internal A•C mismatches in DNA: sequence dependence and pH effects. *Biochemistry*, **37**, 9435–9444.
51. Somerville,L., Krynetski,E.Y., Krynetskaia,N.F., Beger,R.D., Zhang,W., Marhefka,C.A., Evans,W.E. and Kriwacki,R.W. (2003) Structure and dynamics of thioguanine-modified duplex DNA. *J. Biol. Chem.*, **278**, 1005–1011.
52. Bohon,J. and de los Santos,C.R. (2003) Structural effect of the anticancer agent 6-thioguanine on duplex DNA. *Nucleic Acids Res.*, **31**, 1331–1338.

53. Terato,H., Masaoka,A., Asagoshi,K., Honsho,A., Ohyama,Y., Suzuki,T., Yamada,M., Makino,K., Yamamoto,K. and Ide,H. (2002) Novel repair activities of AlkA (3-methyladenine DNA glycosylase II) and endonuclease VIII for xanthine and oxanine, guanine lesions induced by nitric oxide and nitrous acid. *Nucleic Acids Res.*, **30**, 4975–4984.
54. Hitchcock,T.M., Dong,L., Connor,E.E., Meira,L.B., Samson,L.D., Wyatt,M.D. and Cao,W. (2004) Oxanine DNA glycosylase activity from Mammalian alkyladenine glycosylase. *J. Biol. Chem.*, **279**, 38177–38183.
55. Nakano,T., Terato,H., Asagoshi,K., Masaoka,A., Mukuta,M., Ohyama,Y., Suzuki,T., Makino,K. and Ide,H. (2003) DNA-protein cross-link formation mediated by oxanine. A novel genotoxic mechanism of nitric oxide-induced DNA damage. *J. Biol. Chem.*, **278**, 25264–25272.
56. Nakano,T., Katafuchi,A., Shimizu,R., Terato,H., Suzuki,T., Tauchi,H., Makino,K., Skorvaga,M., Van Houten,B. and Ide,H. (2005) Repair activity of base and nucleotide excision repair enzymes for guanine lesions induced by nitrosative stress. *Nucleic Acids Res.*, **33**, 2181–2191.